CAV2021
11th International Symposium on Cavitation
May 10-13, 2021, Daejon, Korea

Detached Eddy Simulation of the Cavitating Flow in a Large-Scale Vaned-Voluted Centrifugal Pump

Zhaoheng Lu [1, 2], Ruofu Xiao [1, 2], Ran Tao [1, 2*] and Weichao Liu [3]

[1] College of Water Resources and Civil Engineering, China Agricultural University, China
[2] Beijing Engineering Research Center of Safety and Energy Saving Technology for Water Supply Network System, China Agricultural University, China
[3] Dongfang Electric Machinery Co., Ltd., China

Abstract: The large-scale vaned-voluted centrifugal pump suits large flow rate and high head. However, the negative impact caused by cavitation will be greater than that of ordinary pumps due to larger energy content. In this study, Detached Eddy Simulation is used to simulate the cavitating flow in a large-scale vaned-voluted centrifugal pump at the design point. The results show that, from the initial cavitation point to the critical cavitation point, the biggest change of cavitation is the scale. The cavitation on blade leading edge will gradually increase. The cavity shape will become more and more unstable with periodic separation. The volume of cavitation is monitored under critical cavitation condition. It may aggravate the complexity of pressure pulsation in downstream components. Therefore, it is necessary to strictly control the cavitation scale to avoid the pump system falling into unstable operation and suffering damage. This study has great significance to the operation stability and security of large water diversion projects.

Keywords: large-scale pump, cavitation, vapor fraction, two-phase flow, flow pulsation

1. Introduction

Large-scale vaned-voluted centrifugal pump is widely applied in water transfer projects. Because of the large flow rate and high head, cavitation scale is larger than common centrifugal pumps under the same conditions [1]. To avoid unnecessary noise, vibration and material damage, the cavitation performance should be strictly checked. Based on the critical cavitation standard, the cavitation-free operation is difficult to achieve [2]. Cavitation bubbles, which are relatively stable and not affective on pump performance, will be a potential factor that induce cavitation erosion on impeller [3]. Therefore, the inception cavitation standard will be more suitable for large-scale vaned-voluted pumps. Some researchers have studied the inception cavitation on pump-turbines [4,5]. The inception cavitation is found related to local flow striking and separation with pressure drop. However, pump-turbine runner usually has a higher blade number than centrifugal pump [6]. The leading-edge local flow of centrifugal pump will be different and need further studies. The cavitation's development will be interesting and meaningful to understand.

In this study, a large-scale vaned-voluted centrifugal pump is studied based on numerical simulation. As computational fluid dynamics (CFD) is proved accurate in evaluate turbomachinery flow [7], it is able to simulate the cavitating multiphase flow from inception cavitation to critical cavitation. Detached Eddy Simulation is used in this study with good resolution of turbulent flow and also save computational costs [8]. The pulsation of cavitation bubbles and vapor volume fractions are monitored to have a better understanding of the leading-edge cavitation of large-scale vaned-voluted centrifugal pump unit.

2. Research objectives and methods

The research objective is a large-scale vaned-voluted centrifugal pump. The design flow rate Q_d is 0.289 m^3/s. The design head H_d is 20.58 m. The design rotational Speed n_d is 1200 r/min. The impeller has 7 blades and the guide vane has 15 blades. The impeller inlet and outlet diameters are 280 mm and 392 mm. The specific speed $n_q=n_d\sqrt{Q_d}/H_d^{3/4}$ is 66.8. The dimensionless coefficient of head is $\psi=2gH/\omega^2R_{iout}^2$ where H is

* Corresponding Author: Ran Tao, randytao@cau.edu.cn

head, Q is flow rate, g is the acceleration of gravity, ω is the rotation angular speed, R_{iout} is the impeller outlet radius. The cavitation coefficient is $\sigma=(p_\infty-p_v)/\rho gH+v_\infty^2/2gH$ where p_∞ is the reference pressure at inlet, p_v is the saturation pressure, v_∞ is the reference velocity at inlet, ρ is the medium density.

CFD simulation is used to simulate the cavitating flow. Detached Eddy Simulation (DES) [9] is used with the shear stress transport (SST) turbulence model. ZGB model [10] is used as the cavitation model. The design flow rate condition is studied. The critical cavitation point (head drop by 1%) is discussed for the pulsation of cavitation. The flow domain includes four parts that inlet, impeller, guide vane and volute as shown in Fig. 1. Hexahedral elements are used for the grid. The mesh node number is 3665088.

In CFD setup, the impeller is defined as rotational and others are stationary. Environment pressure is set as 101325 Pa with the saturation pressure of 3169 Pa. The two phases of fluid are water and water vapor at 25 °C. A mass flow inlet boundary is set at the pump inflow and a static pressure outlet boundary is set at the pump outflow. The outflow pressure can be adjusted to control and simulate different cavitation status. All the walls are non-slip wall boundaries. General grid interface (GGI) is used as a grid connection between each two domains. The convergence criterion is the root mean square residual (RMS) less than 1×10^{-5}. The steady CFD result is set as the initial condition. The following transient simulation simulates 7 impeller revolutions with 720 steps per revolution and 20 iterations per time step.

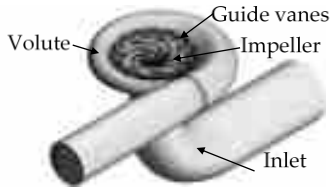

Figure 1. Schematic map of flow domain and mesh

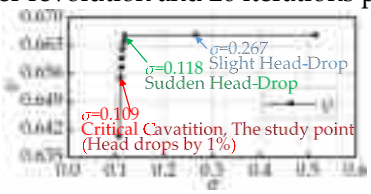

Figure 2. Cavitation performance by CFD

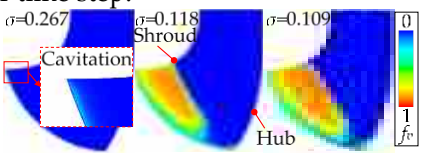

Figure 3. f_v on blade suction surface in meridional view at different σ conditions

3. Results and Discussion

3.1 Cavitation Performance

A cavitation performance is shown in detail as shown in Fig. 2. The cavitation process can be defined as three stages. Firstly, ψ is almost unchanged constant until σ drops to 0.267. Secondly, ψ slightly decreases while σ is between 0.118 and 0.267. Thirdly, when σ is below 0.118, ψ suddenly dropped to a much lower level. There is a sudden drop of ψ and a sudden increasing of cavitation scale. It is unusual in common centrifugal pumps. The development of cavitation and the pressure distributions should be discussed.

3.2 Development of Cavitation

To describe the scale of the cavitation, the specific vapor volume in impeller domain can be defined as $V_s=V_v/V_f$ where V_v is the vapor volume in impeller, V_f is the flow domain volume of impeller. There are three stages as shown in Fig. 2 and Fig. 3. f_v is the cavitation vapor volume fraction within 0~1. At the first stage, there is almost cavitation-free. ψ is almost unchanged. ψ begins to drop slowly when σ is 0.267. The vapor appears on the leading edge of blade near shroud. V_S is about 0.2%. f_v is below at 23%. At the second development stage, the cavitation scale increases. When σ is 0.118, the vapor covers on the blade suction surface near inlet. The cavitation diffuses towards hub and downstream. V_S is about 12.8%. The maximum f_v is 90%. At the third development stage, ψ drops quickly at the point of σ=0.109 is that head drops by 1%. This point is always called the critical cavitation point. The vapor distribution is similar to σ=0.118 especially near shroud. But the cavitation area is larger at the middle of SS. There is cavitation on the blade pressure side (PS). V_S is about 23.75%. The maximum f_v is 92%. As shown in Fig. 4, the scale of cavitation increases from σ=0.267 to σ=0.118. The vapor diffuses from shroud to hub, from leading edge to trailing

* Corresponding Author: Ran Tao, randytao@cau.edu.cn

edge. There are different vapor distributions on different blades and in different channels. When ψ drops rapidly, the cavitation scale is still expanding. Vapor separation can be obviously seen especially on shroud.

3.3 Pressure Distribution on Blade

To understand the reason why cavitation occurs, pressure distributions on blade at cavitation-free condition is analyzed as shown in Fig. 5. Three spanwise positions including 10%, 50% and 90% are plotted. The dimensionless pressure is defined as $C_p=(p-p_\infty)/\rho\omega^2 R_{iout}^2$ where p is pressure. Radius R is also normalized as $C_R=R/R_{iout}$. As observed in Fig. 5, on suction side, C_p near hub is much higher than that on mid-span and near shroud. C_p near shroud increases faster than that on mid-span. The cavitation develops easily at the middle of suction side. Vapor separates easily at the suction side near shroud.

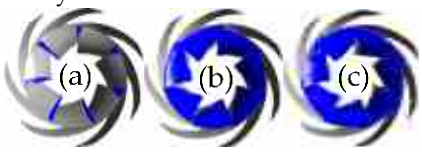

Figure 4. f_v>0.01 in axial view from impeller inlet direction (a) σ=0.267, (b) σ=0.118, (c) σ=0.109

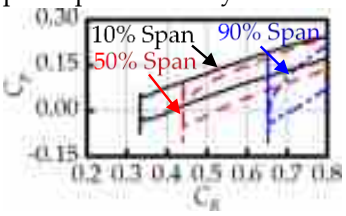

Figure 5. C_p distributions on blade under cavitation-free condition

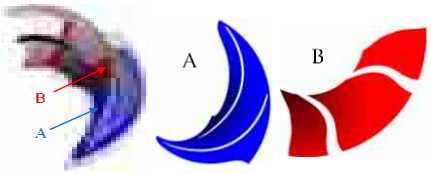

Figure 6. Schematic map of PTN

4. Tracking of Cavitation Variation

4.1 Pulsation Tracking Network (PTN) Method and Setup

Aiming at the critical cavitation condition (σ=0.109) which is important, pulsation tracking network (PTN) method is applied. It tracks the pulsation by arranging large-amount well-organized monitoring points to visualizing the frequency domain characteristics. To analyze the internal cavitation mechanism of the flow field, PTN is set on two positions. As shown in Fig. 6, one is the 50%-span surface (A). To observe vapor frequency domain characteristics from shroud to hub, another is the cross section surface (B) perpendicular to A, shroud and hub. Surface (B) crosses the postion that f_v relatively high. There are 8235 points on A and 3270 points on B.

4.2 Temporal Spatial States

Figure 7 shows the average vapor volume fraction f_v in critical cavitation condition. Vapor is mainly located at the first third of blade SS and near to 50%-span. Vapor diffuses to the next blade PS on shroud and there was a local separation. Vapor accumulates in the middle of the channel on shroud and on the SS-hub connection. In the tail of the cavitation region, vapor separates from blade SS.

Commonly, cavitation is a growing and collapsing process. Vapor changes periodically with certain frequencies as shown in Fig. 8. The dominating frequencies are denoted as f_m. As shown, the dominating cavitation frequencies are mainly 20 Hz and 40 Hz. They are equal to the rotating frequency and its second harmonic frequency. The frequency of 40 Hz distributes in two regions. One is the high vapor volume fraction region near the upstream position of surface A. Another is the high vapor volume fraction region near hub at surface B. This means that the vapor is unstable in these regions. The reason could be the cavitation growing rapidly in these regions and diffusing to the downstream regions. However, the maximum vapor volume fraction amplitude is small (only 0.079) when frequency is 40 Hz. As known, the small-amplitude pulsation of cavitation bubbles is relatively stable without strong damage on impeller.

Another main frequency is 20 Hz. Its coverage region overlaps the cavitation region. These regions are without strong pulsation as shown in Fig. 9. High-amplitude vapor volume fraction distributes around the cavitation region especially near downstream, in the middle of shroud and near SS-shroud connection. In

* Corresponding Author: Ran Tao, randytao@cau.edu.cn

these regions, the average vapor volume fraction is about 0.5. And the maximum vapor volume fraction amplitude is 0.4. This is relatively undesirable because the bubbles are much easier to collapse.

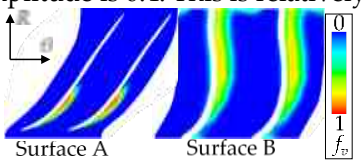

Figure 7. The average vapor volume fraction in critical cavitation condition

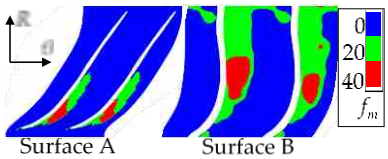

Figure 8. Main frequency distribution

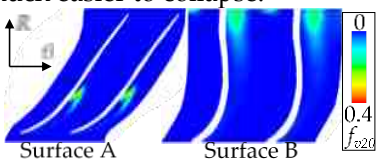

Figure 9. Vapor volume fraction amplitude distribution of 20 Hz

5. Conclusions

Firstly, from the initial cavitation point to the critical cavitation point, the strongest change of cavitation is the scale. Cavitation on blade leading edge will gradually increase. The separation of cavitation first appeared in the middle of blade suction side near shroud. Vapor diffuses from shroud to hub and from leading edge to downstream. The cavitation shape becomes unstable and appears as periodical separation with the drop of cavitation coefficient σ. Secondly, the main frequency of vapor is 20 Hz at critical cavitation point. Vapor accumulates in the middle of the blade channel near shroud and near SS-hub connection. The edge of cavitation bubble region has low vapor volume fraction and high variation amplitude. It represents frequent collapse of bubble which may easily causes cavitation erosion damage on materials. In general, this study will be helpful in enhancing the cavitation performance of large-scale pumps.

Acknowledgments: The authors would like to acknowledge the support of National Natural Science Foundation of China. This study is funded by National Natural Science Foundation of China grant number 51909131.

References

1. Tao, R.; Xiao, R.; Wang, F.; et al. Cavitation behavior study in the pump mode of a reversible pump turbine. *Renewable Energy* **2018**, *125*, 665-667.
2. International Electrotechnical Commission. *Hydraulic Turbines, Storage Pumps and Pump-Turbines-Model Acceptance Tests*, 2nd ed.; International Standard IEC 60193: Lausanne, Switzerland, 1999.
3. Zhang, W.; He, X.; Wang, X.; et al. Numerical Simulation of Cavitation Flow in a Centrifugal Pump. 2nd International Conf. on Advances in Computational Modeling and Simulation, Kunming, China, July 17-19, 2013.
4. Anciger, D.; Jung, A.; Aschenbrenner, T. Prediction of Rotating Stall and Cavitation Inception in Pump Turbines. 25th IAHR Symposium on Hydraulic Machinery and Systems, Timisoara, Romania, September 20-24, 2010.
5. Jese, U.; Fortes-Patella, R.; Antheaume, S. High Head Pump-turbine: Pump Mode Numerical Simulations with a Cavitation Model for Off-design Conditions. 27th IAHR Symposium on Hydraulic Machinery and Systems, Montreal, Canada, September 22-26, 2014.
6. Zhu, D.; Xiao, R.; Tao, R.; et al. Impact of Guide Vane Opening Angle on the Flow Stability in a Pump-Turbine in Pump Mode. *Proc. of the IMechE Part C-Journal of Mechanical Engineering Science* **2017**, *231(13)*, 2484-2492.
7. Tao, R.; Xiao, R.; Yang, W.; et al. Optimization for Cavitation Inception Performance of Pump-Turbine in Pump Mode Based on Genetic Algorithm. *Mathematical Problems in Engineering* **2014**, *2014*.
8. Spalart, P.R.; Jou, W.; Strelets, M.; et al. High Comments on the Feasibility of LES for Wings, and on a Hybrid RANS/LES Approach. 1st International Conference on DNS/LES, Ruston, USA, 1997.
9. Strelets, M. Detached Eddy Simulation of Massively Separated Flows. 39th AIAA Aerospace Sciences Meeting and Exhibit, Reno, NV, USA, January 8-11, 2001.
10. Zwart, P.J.; Gerber, A.G.; Belamari, T. A Two-phase Flow Model for Predicting Cavitation Dynamics. 5th International Conference on Multiphase Flow, Yokohama, Japan, 2004.

* Corresponding Author: Ran Tao, randytao@cau.edu.cn